ELSEVIER

Data Article

Electromyometrial imaging dataset of electromyograms and isochrone maps under deformation/electrical noise contaminations

Hui Wang [a, b, c], Wenjie Wu [b, c, d], Michael Talcott [e],
Robert C. McKinstry [f], Pamela K. Woodard [d, f],
George A. Macones [g], Alan L. Schwartz [h], Phillip Cuculich [i],
Alison G. Cahill [g, **], Yong Wang [b, c, d, f, *]

[a] Department of Physics, Washington University, St. Louis, MO, 63130, USA
[b] Center for Reproductive Health Sciences, Washington University, St. Louis, MO, 63130, USA
[c] Department of Obstetrics & Gynecology, School of Medicine, St. Louis, MO, 63110, USA
[d] Department of Biomedical Engineering, Washington University, St. Louis, MO, 63130, USA
[e] Division of Comparative Medicine, Washington University, St. Louis, MO, 63110, USA
[f] Mallinckrodt Institute of Radiology, Washington University School of Medicine, St. Louis, MO, 63110, USA
[g] Department of Women's Health, University of Texas at Austin, Austin, TX, 78712, USA
[h] Department of Pediatrics, Washington University School of Medicine, St. Louis, MO, 63110, USA
[i] Department of Cardiology, Washington University School of Medicine, St. Louis, MO, 63110, USA

A R T I C L E   I N F O

A B S T R A C T

The dataset presented in this paper is related to the recent work "*Accuracy of electromyometrial imaging of uterine contractions in clinical environment*" [1]. The dataset including body-uterus geometry obtained from magnetic resonance imaging (MRI), uterine electrograms and isochrone maps reconstructed using Electromyometrial imaging (EMMI) under various levels of deformations and electrical noise contamination in a translational sheep model are reported. The dataset make it possible for detailed evaluation and further improvement of EMMI. In addition, the researchers working on other types of electrophysiology imaging techniques, such as electrocardiographic imaging (ECGI), and Electrogastrography imaging (EGGI) could also adopt our method [1] and

employ the dataset to evaluate and improve their imaging techniques.

Specifications Table

|	
Subject	Biomedical Engineering
Specific subject area	Electrophysiology; Imaging technique
Type of data	Figures
How data were acquired	Body-uterus geometry was imaged by Magnetic resonance imaging (MRI) and segmented using Amira software (Version 6.2). Electrograms and isochrone maps under deformation or electrical noise were reconstructed by Electromyometrial imaging (EMMI).
Data format	Raw computational Analyzed
Parameters for data collection	Images of uterus and abdomen were acquired using human MRI scanner from an anesthetized sheep. The sheep uterine electrograms were recorded during a surgical procedure to expose the sheep uterus [2]. Laplacian deformation algorithm was employed to simulate and generate geometrical changes under ideal elastic deformation conditions.
Description of data collection	MRI images of uterus and abdomen were acquired using a radial VIBE fast T1-weighted sequence from an anesthetized sheep. MRI images were segmented and rendered to uterus and body mesh. The sheep uterus was exposed surgically, and an elastic sock containing 64 or 128 sintered Ag−AgCl electrodes was slipped over the uterus to record the electrograms at a 2 kHz sampling rate using Biosemi system [2]. Gaussian and Perline noise were simulated with the SNR = 17.5 dB. Maximum body-uterus deformation ratios simulated for Type I kick, Type II kick, contraction were 0.3, 0.3, 0.14, respectively. The standard deviation of deformation distance of fetal/maternal movements is 0.67 cm.
Data source location	Washington University in St. Louis School of Medicine, St. Louis, Missouri, United States
Data accessibility	The data are available with the article.
Related research article	H. Wang, W. Wu, M. Talcott, S. Lai, R.C. McKinstry, P.K. Woodard, G.A. Macones, A.L. Schwartz, P.S. Cuculich, A.G. Cahill, Y. Wang, Accuracy of electromyometrial imaging of uterine contractions in clinical environment, *Computers in biology and medicine*, 116 (2020) 103543. doi:10.1016/j.compbiomed.2019.103543. [1].

Value of the Data
- The computational and processed data will enable readers to reproduce all our findings [1], and more importantly allow peer researchers to use the data as benchmarking to improve EMMI technique.
- The data and simulation of geometrical changes can also be adapted to assess the accuracy of other types of electrophysiology imaging methods, such as electrocardiographic imaging (ECGI) [3], Electrogastrography imaging [4], etc.
- Readers and researchers can take our work as the base and continue to incorporate more realistic geometrical deformation models and electrical noises to generate insights about the clinical EMMI translation and data interpretation.

1. Data

The dataset shows the pregnant sheep body-uterus geometry (Fig. 1), different types of electrical noise (Fig. 2), different types of geometrical deformations (Fig. 3), EMMI-reconstructed electrograms (Fig. 4), and isochrone maps (Fig. 5) under various geometrical deformations and electrical noises.
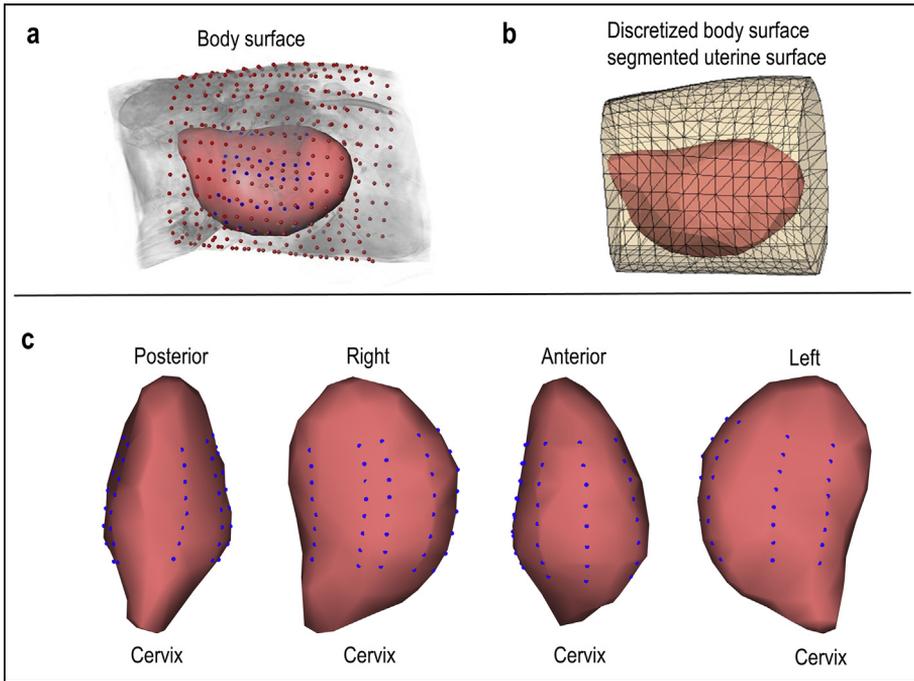
Fig. 1. Body-uterus geometry. **a**, Sheep body-uterus geometry with unipolar electrode locations, red dots represent body surface electrode locations and blue dots represent uterine surface electrode locations. **b**, Discretized body-uterus geometry implemented in the analysis [1]. **c**, Full uterine surface recorded from MRI (pink) and uterine surface electrode locations (Blue dots).
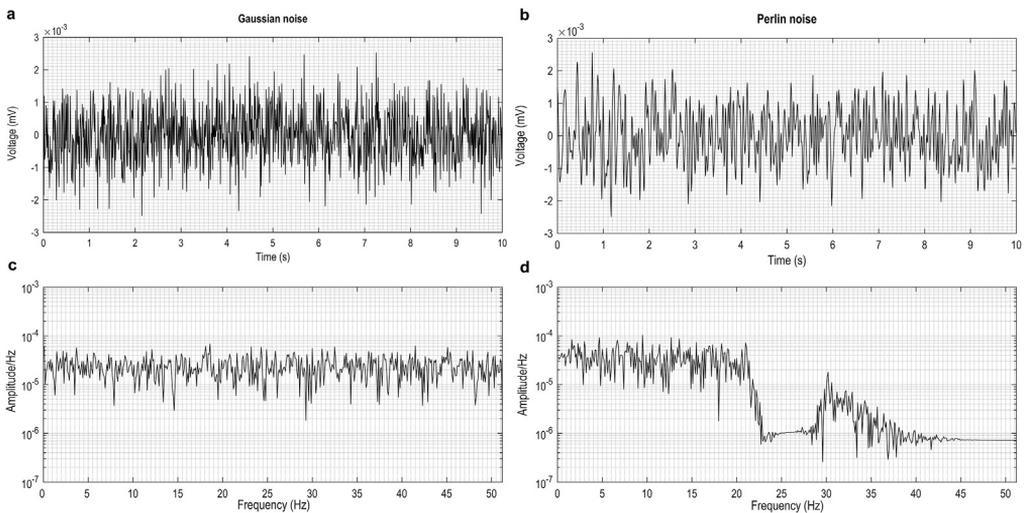

Fig. 2. Gaussian and Perlin noise. a, b Simulated noise electrogram of the first 10 seconds of one electrode at SNR = 17.5 dB. **c, d** noise amplitude per Hz of electrograms in a, b. The total noise power is 7.49×10^{-4} mW in a and 7.35×10^{-4} mW in b. The total noise power under 10 Hz is 7.1×10^{-8} mW in a and 1.9×10^{-7} mW in **b**.
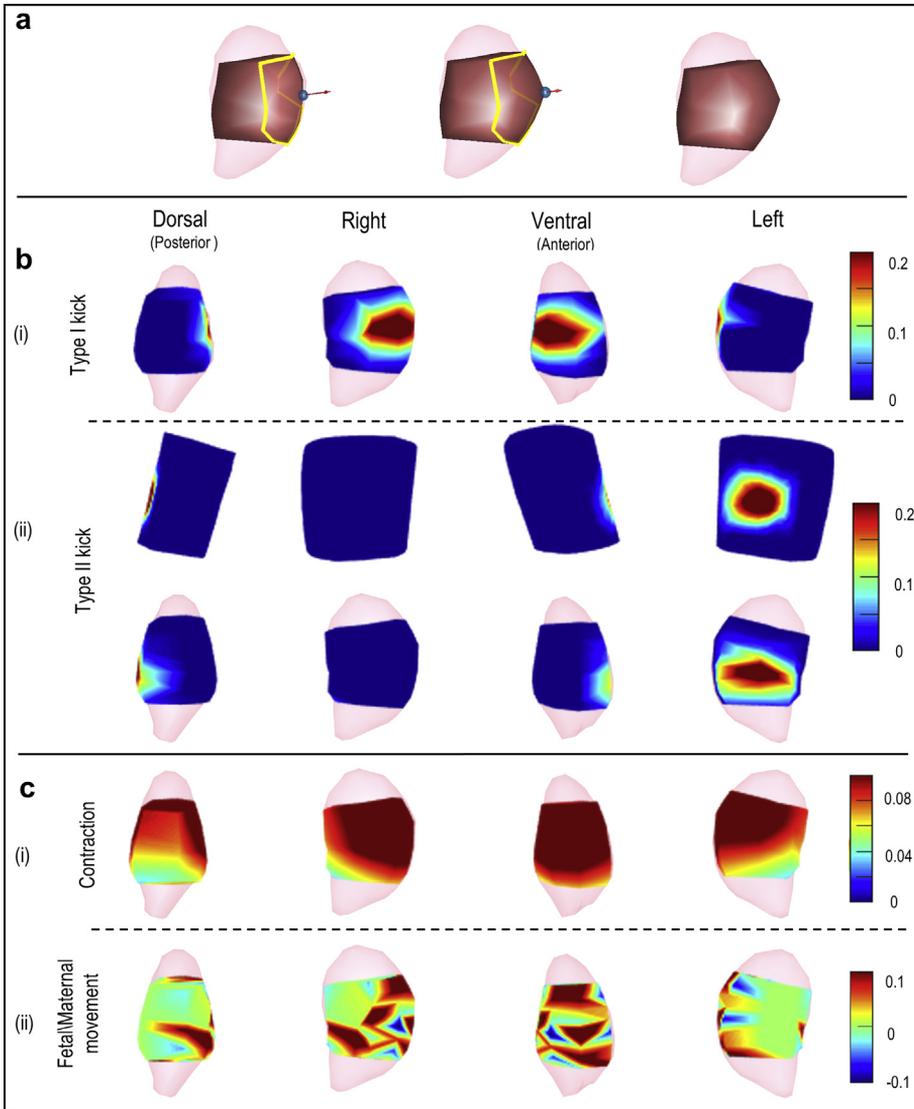
Fig. 3. Type I deforming process and extreme deformation ratio distribution. a, Type I deforming processing. As for Laplacian deformation algorithm, a chosen handle was moved to represent the kick center (blue sphere), a kick direction was defined as outwards from the center of the uterus (red arrow), and a non-stationary area was defined as deformed (the area from yellow belt to the center). **b, c** local and global deformation, respectively. In each row, the four images show deformation ratios in heat maps from the four indicated views. Warm colors indicate large deformations, and cool colors indicate small deformations as indicated in scales at far right.
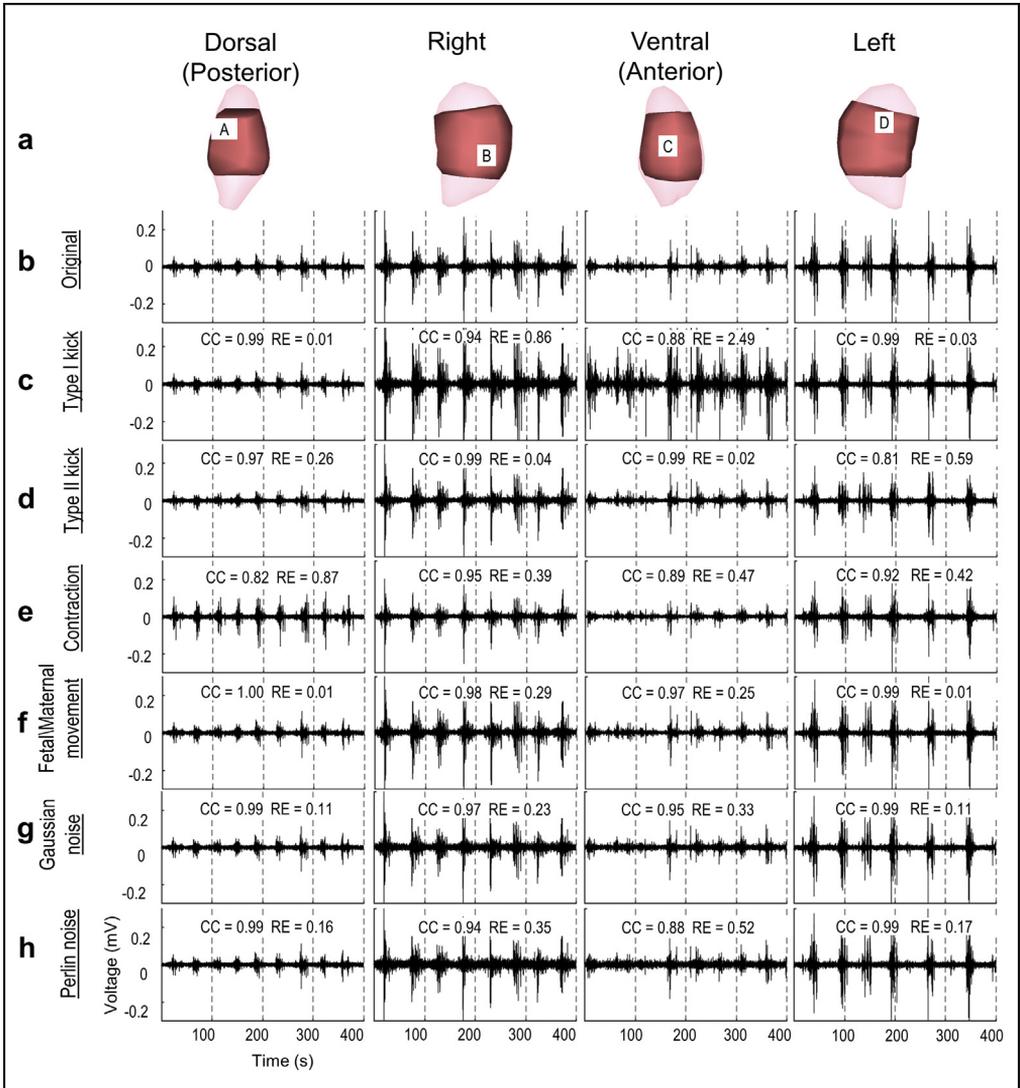
Fig. 4. Electrograms under extreme deformations or noise. a, Four views of sheep uterus; light pink is the uterine geometry segmented from MRI images; dark pink is the discretized uterine geometry from the locations of electrodes placed on the uterine surface. **b**, Electrograms reconstructed from original body surface potentials from four locations labeled A, B, C, and D in **a**. **c**–**h**, Reconstructed electrograms corresponding to the deformed or noise-contaminated body surface potentials. Deformation extents are at the extreme conditions, and SNR = 12.5 dB.
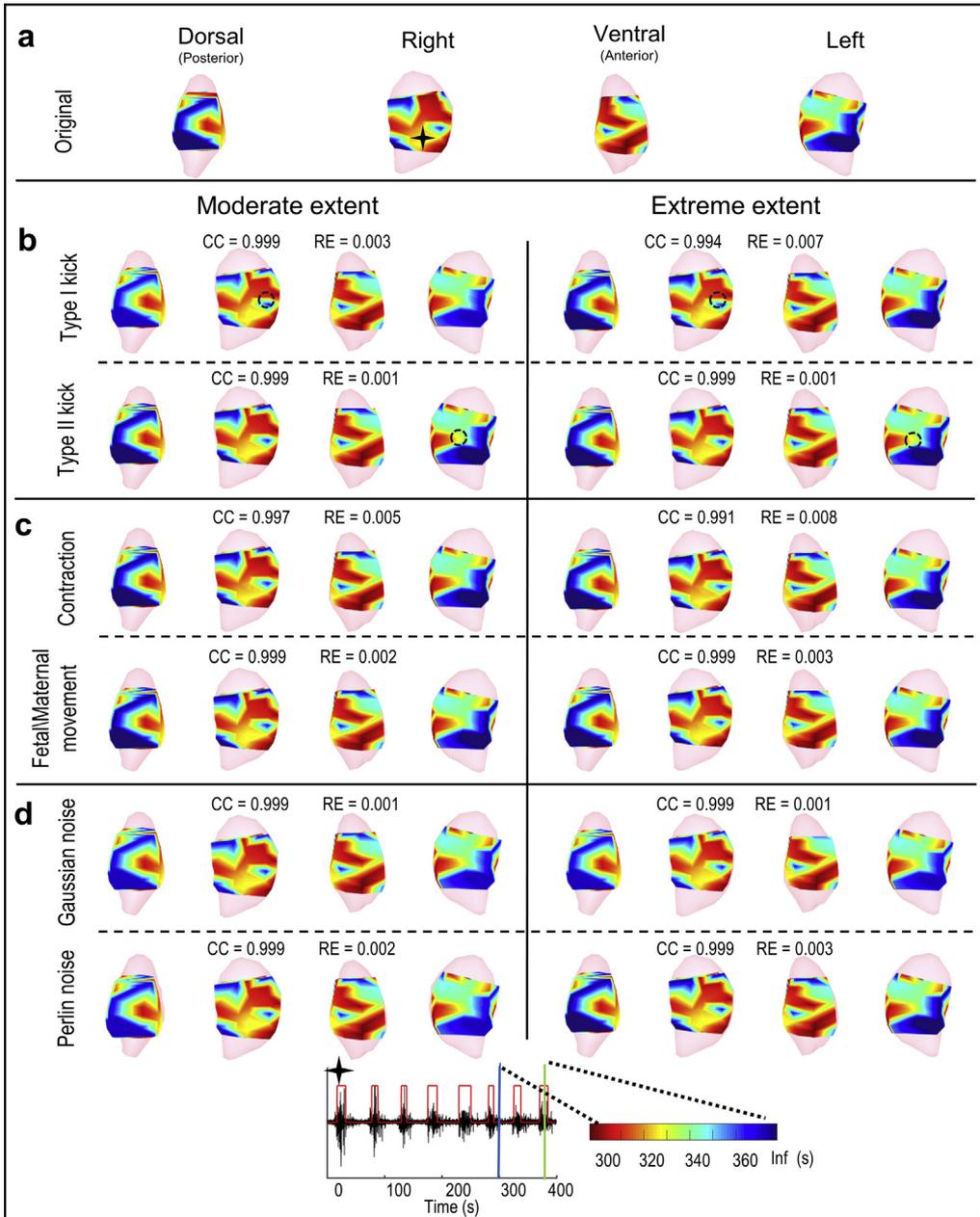
Fig. 5. EMMI-reconstructed isochrone maps during another EMG burst. In the top seven rows, isochrones are displayed for two deformation or noise levels and shown in four views. In the heat maps, red indicates early activation, blue indicates late activation, and the darkest blue denotes regions in which no activation was recorded during the specific observation window. The black star indicates the location at which the electrogram (bottom row) was reconstructed. The electrogram shows EMG bursts (denoted by the red step lines); blue and green vertical lines indicate the start and end of the observation window for EMG burst (from 286 s to 378 s). a - d, Isochrones from original, local deformed, global deformed, and noise-contaminated electrograms, respectively. Black circles in panel b mark local deformation centers.

These data were employed to evaluate the accuracy of EMMI in real complicated clinical environments and maternal/fetal motions [1].

2. Experimental design, materials, and methods

The experiment used Katahdin sheep as a model for human pregnancy considering their similar abdomen size as humans and respond to steroids to induce labor [2,5]. The sheep with gestation age around 140−145 days were obtained from the local farm. 24−48 hours before the MRI, sheep was intramuscularly administered with 16 mg dexamethasone. 1−2 hours before the MRI, sheep was shaved free of hair at the level of pelvis. Up to 256 MRI markers were applied around the lower abdomen and back of the sheep. MRI images were acquired from a 3T Siemens Prisma with radial volume interpolated breath-hold examination fast T1-weighted sequence. The resolution of the image is 1 mm × 1 mm x 3 mm. The body-uterus geometry (Fig. 1) was segmented from MRI images using Amira software. After the MRI, the sheep was transferred to operating room, where the uterine surface electrograms were recorded from up to 128 Biosemi unipolar electrodes. The detailed experiment procedure was reported in the previous work [1,2].

Gaussian and Perline noise were simulated with the SNR = 17.5 dB (Fig. 2). Body-uterus deformations were simulated and the maximum deformation ratios of Type I kick, Type II kick, contraction were 0.3, 0.3, 0.14, respectively. The standard deviation of deformation distance of fetal/maternal movement is 0.67 cm (Fig. 3). Combined the simulated noise and geometrical deformations with the measured uterine surface electrograms, the contaminated uterine surface electrograms were calculated (Fig. 4). The activation times of EMG burst near 300-s were calculated and assembled to the isochrone maps (Fig. 5).

Conflict of Interest

The authors declare that they have no known competing financial interests or personal relationships that could have appeared to influence the work reported in this paper.

References

[1] H. Wang, M. Wu, M. Talcott, S. Lai, R.C. McKinstry, P.K. Woodard, G.A. Macones, A.L. Schwartz, P.S. Cuculich, A.G. Cahill, Y. Wang, Accuracy of electromyometrial imaging of uterine contractions in clinical environment, Comput. Biol. Med. 116 (2020) 103543, https://doi.org/10.1016/j.compbiomed.2019.103543.

[2] W. Wu, H. Wang, P. Zhao, M. Talcott, S. Lai, R.C. McKinstry, P.K. Woodard, G.A. Macones, A.L. Schwartz, A.G. Cahill, P.S. Cuculich, Y. Wang, Noninvasive high-resolution electromyometrial imaging of uterine contractions in a translational sheep model, Sci. Transl. Med. 11 (2019) eaau1428, https://doi.org/10.1126/scitranslmed.aau1428.

[3] P.R. Johnston, Accuracy of electrocardiographic imaging using the method of fundamental solutions, Comput. Biol. Med. 102 (2018) 433−448, https://doi.org/10.1016/J.COMPBIOMED.2018.09.016.

[4] A.A. Allegra, A.A. Gharibans, G. Schamberg, D.C. Kunkel, T.P. Coleman, Bayesian inverse methods for spatiotemporal characterization of gastric electrical activity from cutaneous multi-electrode recordings, PLoS One 14 (2019), https://doi.org/10.1371/journal.pone.0220315.

[5] J.S. Barry, R.V. Anthony, The pregnant sheep as a model for human pregnancy, Theriogenology 69 (2008) 55−67, https://doi.org/10.1016/j.theriogenology.2007.09.021.